Nanoscale

COMMUNICATION

Cite this: Nanoscale, 2014, 6, 7842

Received 10th April 2014
Accepted 9th May 2014

DOI: 10.1039/c4nr01934b

www.rsc.org/nanoscale

An electrospun nanowire-based triboelectric nanogenerator and its application in a fully self-powered UV detector†

Youbin Zheng,‡[a] Li Cheng,‡[a] Miaomiao Yuan,[ab] Zhe Wang,[a] Lu Zhang,[a] Yong Qin*[ac] and Tao Jing[b]

A new kind of triboelectric nanogenerator (TENG) is developed based on electrospun PVDF and nylon nanowires. This nanogenerator exhibits the remarkable characteristics of easy fabrication, low cost and high output. Its open-circuit voltage and short-circuit current density respectively reach up to 1163 V and 11.5 μA cm^{-2} driven by the vibration with a triggering frequency of 5 Hz and an amplitude of 20 mm. The peak power density is 26.6 W m^{-2}. It directly powered a DC motor without an energy storage system for the first time. By harvesting energy from the environment using this TENG, a fully self-powered UVR detection device is developed to show the level of UVR directly without additional components.

Introduction

Over the last few decades, energy crisis has become a global concern and researchers have been making every effort to search for green and renewable energy sources. Harvesting mechanical energy from the environment and biological systems has attracted increasing attention for powering personal electronics. As an emerging technology for mechanical energy harvesting, triboelectric nanogenerators (TENGs) have been recently developed as effective candidates for converting mechanical energy in the environment into electrical energy for self-powered devices and systems by a conjunction of tribo-electrification and electrostatic induction.[1–4] It has been demonstrated that the output performance of the TENGs depends intimately on the properties of their component materials, such as types[5] and surface structures[6–8] of the materials. Until now, different preparation methods, such as patterned silicon templates made by a complicated procedure,[6–9] a typical photolithography process[9] and a dry-etching process,[10,11] have been developed to fabricate TENGs composed of various materials. But most of these methods are complex and time-consuming, which limits TENGs' potential applications. From a practical point of view, a highly simple method to fabricate a TENG with superior performance is urgently needed.

On the other hand, although TENGs have been utilized in power sensors to detect mercury ions,[12] pressure,[13] wind vectors,[14] active vibration[15] and so on, most of these sensors need to work with the expensive and high-precision electric measurement equipment,[13–16] which will make the sensors hard to be used in some particular situations. Furthermore, self-powered portable UV detectors are beneficial for protecting people from UV light damage. Up to 60 000 deaths are caused by too much exposure to ultraviolet radiation (UVR) worldwide each year and most of the UV-related illnesses and deaths can be avoided through a series of simple prevention measures, according to the World Health Organization.[17] With increasing awareness among people about the damage of skin from UV exposure, it is greatly significant to design a fully integrated, stand-alone and self-powered UVR level detection device which can display the UVR level anytime and anywhere to alert people to protect their skin when the UV intensity exceeds dangerous limits.

In this work, we have developed a new kind of TENG based on electrospun nanowires (ENTENG). It exhibits the remarkable characteristics of easy fabrication, low cost and high output. The open-circuit voltage and the short-circuit current density of the ENTENG respectively reach up to 1163 V and 11.5 μA cm^{-2} under the vibration with a triggering frequency of 5 Hz and an amplitude of 20 mm. The peak power density is 26.6 W m^{-2}. When it is driven by human footfalls, we got a peak current density as high as 209 μA cm^{-2}. By using this device, we directly powered a DC motor directly without an energy storage system for the first time and developed a fully self-powered UVR

[a]Institute of Nanoscience and Nanotechnology, School of Physical Science and Technology, Lanzhou University, Lanzhou, 730000, China. E-mail: qinyong@lzu.edu.cn

[b]The Research Institute of Biomedical Nanotechnology, School of Basic Medical Sciences, Lanzhou University, Lanzhou, 730000, China

[c]Beijing Institute of Nanoenergy and Nanosystems, Chinese Academy of Sciences, Beijing 100085, China

† Electronic supplementary information (ESI) available: See DOI: 10.1039/c4nr01934b

‡ These authors contributed equally to this work.

detection device that could show the level of UVR directly without additional components. This work expands the potential applications of TENGs in the field of public health.

Results and discussion

As demonstrated in previous studies, rough surfaces with micro/nano structures have a larger effective triboelectric effect and can generate more surface charges during friction.[6–10,18,19] So in this work we have fabricated nanostructures to enhance the friction and improve the output performance of the TENG by the electrospinning method which is well known as one of the most simple, low-cost and versatile methods for producing nanostructured fibers.[20] The schematic diagram of the ENTENG is shown in Fig. 1a. Poly(vinylidene fluoride) (PVDF) and polyamide (nylon) are chosen for their high negativity/positivity in the triboelectric series. An Ag film electrode and PVDF nanofibers are deposited onto two sides of one Kapton film by magnet sputtering and electrospinning as the top plate, and an Ag film electrode and nylon nanofibers are successively deposited onto the same side of the other Kapton film by a similar method as the bottom plate. Owing to the naturally bent structure of Kapton films, these two processed plates of the same size are attached face-to-face to form an arch-shaped ENTENG (Fig. 1a). The surface morphologies of as-spun PVDF and nylon nanofibers are shown in Fig. 1b and c. The electrospun nanofibers with diameters of approximately 790 nm and 550 nm respectively are randomly distributed on the Kapton film. The electricity generation process of the fabricated TENG is schematically depicted in Fig. 1d. When the bending plates are pressed, the top plate and bottom plates contact and rub against each other. As PVDF is much more triboelectrically negative than nylon, electrons are injected from nylon to the PVDF surface, generating positive triboelectric charges on the nylon side and negative charges on the PVDF side. When the ENTENG is released, the contacting surfaces are separated due to resilience. The top Ag electrode possesses a lower electric potential than the bottom Ag electrode, producing an electric potential difference,[10] which will drive the electrons to flow through an external load from the top Ag electrode to the bottom Ag electrode to reach an electrostatic equilibrium. In the meantime, positively induced charges are produced on the top Ag electrode and negatively induced charges on the bottom Ag electrode. Once the TENG is pressed again to make the two plates contact, the redistributed charges will build a reversed potential to drive electrons to flow toward the opposite direction. When a new equilibrium is reached, a cycle of electricity generation is finished.

To investigate the electrical output performance of the ENTENG, we use a linear motor to periodically press and release the device. In order to eliminate the influence of the noise caused by the measurement equipment (voltmeter and amperemeter), we changed the way of the connection of the device with the measurement equipment. As shown in Fig. 2a, the configuration that the positive probe of the measurement system connecting with the PVDF nanofiber membrane and the negative probe connecting with the nylon nanofiber membrane is defined as the forward connection (FC) and the inverted connecting configuration is defined as the reverse connection (RC). According to the working principle of the TENG (Fig. 1d), for the FC, an instantaneous positive–negative current and voltage will be measured when the TENG is driven by a cyclic pressing–releasing movement of the linear motor. Reversely, the negative–positive output current and voltage should be

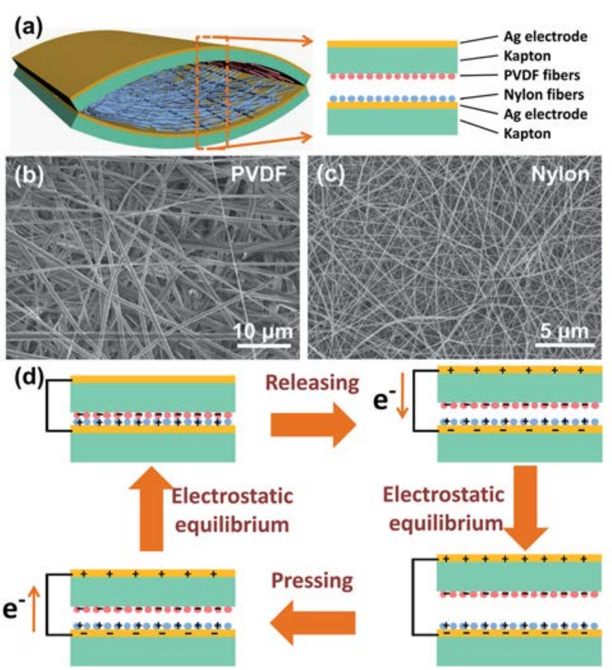

Fig. 1 Structure and working principle of the ENTENG. (a) Schematic of the ENTENG. (b and c) SEM images of the electrospun PVDF and nylon nanofibers. (d) The charge distribution in the device and the flowing direction in the circuit when the device is pressed and released.

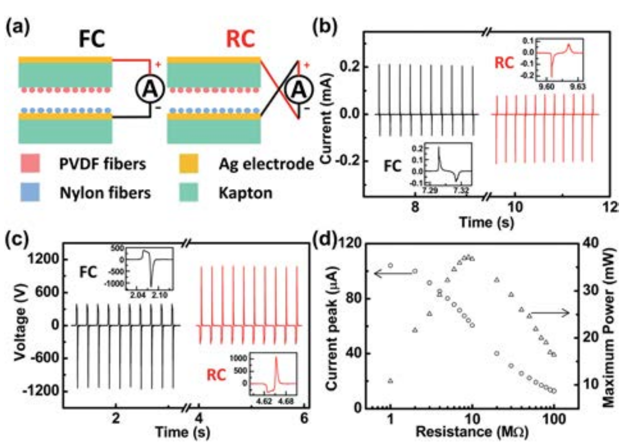

Fig. 2 Output of the ENTENG. (a) Schematic of the forward connection (FC) and reverse connection (RC) which are used to rule out the possible system artifacts. (b and c) Short-circuit current and open-circuit voltage of the ENTENG driven by a linear motor. The black and red curves represent the output signals under the FC and RC, respectively. (d) Current (circle) and power (triangle) of the ENTENG with different load resistants.

measured for the RC. As shown in Fig. 2b and c, driven by the motor movement with a frequency of 5 Hz and an amplitude of 20 mm, the measured output signals are consistent with the above analysis, which means that the output current and voltage are true signals according to the previous work.[21] The short-circuit current (Fig. 2b) and the open-circuit voltage (Fig. 2c) of the ENTENG are 211 μA and 1163 V, respectively. And the corresponding current density is 11.5 μA cm^{-2} and the charges flowing between two electrodes per peak are 0.332 μC, giving the corresponding triboelectric charge density of 179.6 μC m^{-2}. To investigate the effective electric power of the ENTENG, resistors are connected as external loads. As displayed in Fig. 2d, the instantaneous current drops with increasing load resistance due to ohmic loss. As a result, the instantaneous power output ($W = I_{\text{peak}}{}^2R$) reached the maximum value of 37.1 mW at a load resistance of 9 MΩ, corresponding to a power density of 26.6 W m^{-2}. This result indicates that the ENTENG is particularly efficient when the load has a resistance on the order of 10^7 ohms. In addition, the mechanical stability of the ENTENG is investigated. As demonstrated in Fig. S1,† only a slight decline (~5%) is observed for the short-circuit current after a total of 36 000 working cycles.

To check if the electrospun nanowires are beneficial to the output of the TENG, we compared the output of the ENTENG with the TENG composed of smooth surfaces (more details are shown in Fig. S2†). These two TENGs have the same device structure except that the surface morphology of triboelectric materials is different. Fig. 3 shows the short-circuit current of TENGs with a smooth surface and an electrospun nanowire surface measured under the same conditions. The short-circuit currents of the ENTENG and the smooth surface TENG are 81 μA and 19 μA, respectively. Meanwhile, the corresponding inductive charges per peak are 0.351 μC and 0.085 μC. There are 4.3 and 4.1 times increase respectively in short-circuit current and transferred charges. This result shows that the nanowires prepared by the electrospinning method is effective in improving the output of TENGs and can compare favorably with those received based on other existing complex preparation methods.[6,7] Therefore, electrospinning benefits the fabrication of TENG with superior performance and low cost.

To convert the energy of human motion into electricity to power micro/nanosystems, the ENTENG is attached onto a sole to harvest the energy of human walking. Fig. 4a shows that the device produces a peak current of 3 mA when driven by human footfalls, which implies that the output current density is 209 μA cm^{-2}. By using this ENTENG as a direct power source, we successfully powered a DC motor without an energy storage process. The ENTENG is connected to the input end of a bridge rectifier and the DC motor is connected to the output end of the rectifier (Fig. S3†). The alternating current obtained from the ENTENG is converted into direct current by the bridge rectifier. As shown in Fig. 4b and Movie 1 in the ESI,† the motor began to rotate in the clockwise direction when the ENTENG was triggered by hand tapping, and the rotation direction changed to counter clockwise when the DC motor was reversely connected with the output end of the bridge rectifier. So it is feasible to instantaneously drive some commercial DC motors by an ENTENG, which expands the application of the triboelectric nanogenerator.

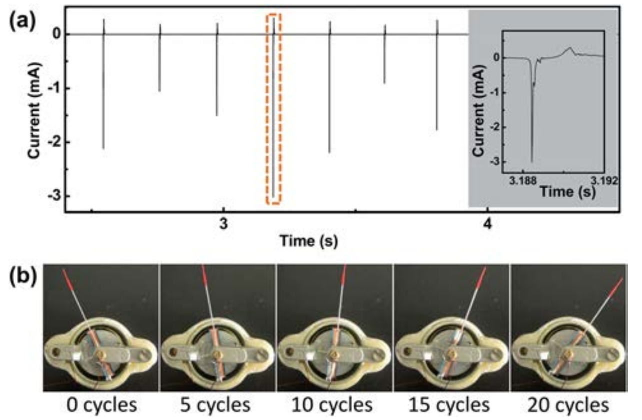

Fig. 4 Collecting the energy of human motion by the ENTENG. (a) Short-circuit current of the ENTENG triggered by human footfalls. The inset shows the details of the highest current peak. (b) Optical images of a DC motor directly driven by hand tapping, which shows the motion of the motor every five working cycles of the ENTENG.

As the output current of the ENTENG changes with the loads of different resistances, it is possible to integrate the ENTENG with a UV sensor to fabricate a self-powered UVR level detection device to detect the UVR levels of low, moderate, high, very high and extreme defined by the World Health Organization.[22] As shown in Fig. 5a and b, an ENTENG is connected in series with a ZnO nanofiber based UV sensor and four LEDs, while shunt resistors are connected in parallel with each LED. The resistances we used are 96.3, 30.6, 22.5 and 17.2 kΩ, corresponding to R_1, R_2, R_3 and R_4, respectively. A series of Zener diodes with the reverse breakdown voltage of 182 V are connected in parallel with the TENG, which are used to provide a stable working voltage and prevent damage to electronics. In this experiment, we tried to automatically warn the five UVR levels by the boundary values of 5, 12.5, 17.5 and 25 W m^{-2}. From the current–time curve of the UV sensor under 1 V bias voltage and different UV light intensities shown in Fig. S4,† the resistance of the UV sensor changes with the light intensity, which results in the change of the current according to Ohm's law. When the UV intensity is higher than the boundary value of different UVR levels, the LED begins to flicker. In this way, the UVR level could be displayed by the number of flickering LEDs. When the UV

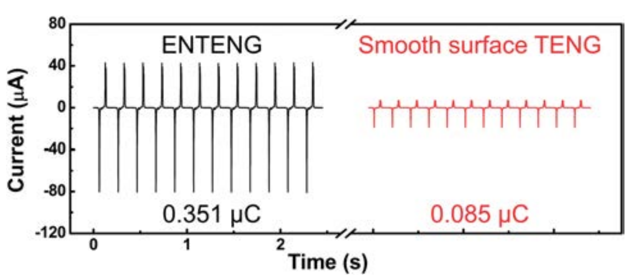

Fig. 3 The output current of the ENTENG and the output current of the smooth surface TENG with a similar device structure.

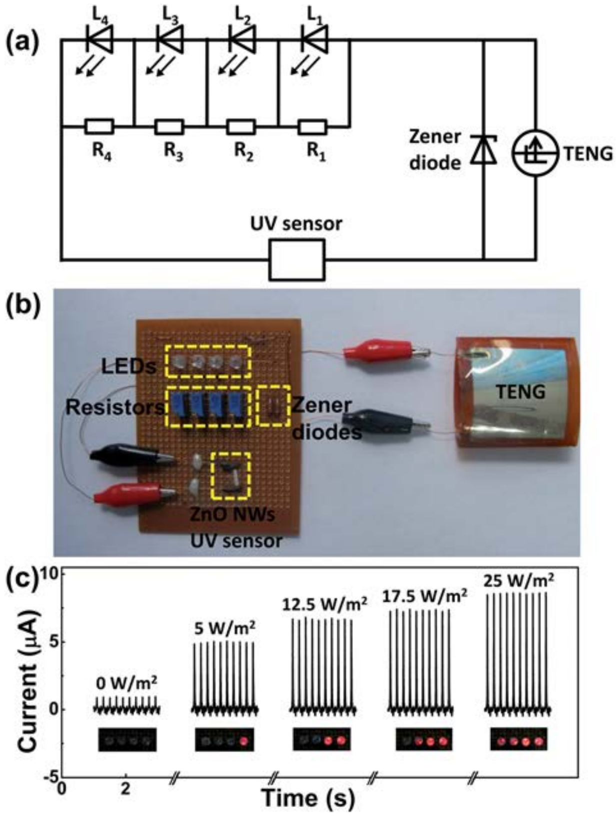

Fig. 5 A self-powered UVR level detection system driven by the ENTENG. (a and b) Schematic and optical images of the UVR level detection system powered by an ENTENG. (c) Current flowing across the UV sensor and the optical images of the LEDs at UV intensities of 0, 5, 12.5, 17.5 and 25 W m^{-2}.

intensity is less than 5 W m^{-2}, the UV sensor has a very high resistance and the current in the circuit is so small that no LED flickers, which means low danger from the UV light. When the UV intensity reaches or exceeds 5 W m^{-2} but is less than 12.5 W m^{-2}, the resistance of the UV sensor decreases because of the increasing carriers so that the corresponding current is increased and one LED flickers, which means moderate risk of harm from unprotected UV exposure. With the increase of UV intensity, more carriers are generated in the ZnO nanowires. So two LEDs flicker which means a high risk of harm when the UV intensity is in the range of 12.5 W m^{-2} to 17.5 W m^{-2}. Analogously, three LEDs flicker means a very high risk of harm (17.5 to 25 W m^{-2}), and four LEDs flicker means an extreme risk of harm (more than 25 W m^{-2}). Fig. 5c shows the optical images of the LEDs and the output current of the ENTENG in the circuit at the UV intensities of 0, 5, 12.5, 17.5 and 25 W m^{-2}. More details are illustrated in ESI Movie 2.† As shown above, the UVR level detection device is very simple and easy to be integrated with the self-powered portable equipment. By using this equipment, anyone can measure the UVR level anytime and take appropriate steps to protect one's skin and eyes. This work not only presents a portable and self-powered UVR level detection device to alert people to a possible over-exposure to UV light, but also expands the applicability of TENGs as power sources for self-sustained electronics.

Conclusions

In summary, based on the electrospinning method, we developed a new way to fabricate the high performance TENG. The ENTENG exhibits the remarkable characteristics of easy fabrication, low cost and high output. Driven by a linear motor at a frequency of 5 Hz and an amplitude of 20 mm, we got a short-circuit current density of 11.5 μA cm^{-2} and an open-circuit voltage of 1163 V. The peak power density is 26.6 W m^{-2}. Attached onto the sole to collect the energy of human motion, the ENTENG produced the highest peak current density of 209 μA cm^{-2} when driven by human footfalls. Moreover, the ENTENG is successfully used to power a DC motor directly by collecting the energy of hand tapping. By using the ENTENG as a power source, we fabricated a fully self-powered and portable UVR level detection device which could measure and display the UVR level directly. This work unambiguously shows the feasibility of the ENTENG for powering portable sensors for health care and other electronic devices.

Experimental section

Preparation of the PVDF and nylon solutions

3.75 g PVDF was mixed with 8.5 g *N*,*N*-dimethylacetamide (DMAC) and 12.75 g acetone in a 50 mL triangular flask. The solution was stirred at 60 °C for 30 min and cooled to room temperature. 2 g nylon was mixed with 4.8 g formic acid and 3.2 g dichloromethane in a 50 mL triangular flask, then it was stirred for 1 h to ensure the dissolution of nylon. All reagents were analytically pure and used without any further purification.

Preparation of PVDF and nylon nanofibers

The experimental setup of electrospinning to fabricate the nanofibers is a horizontal electrospinning setup reported in previous studies.[23] The solution is loaded into a syringe and the distance between the needle and the collector is 16 cm for all the experiments. To prepare PVDF nanofibers, electrospinning is conducted at 15 kV with the feed rate of PVDF solution 3 mL h^{-1}. For nylon, the applied electrospinning voltage is 16 kV and the nylon solution feed rate is 1 mL h^{-1}. All the nanofibers are collected on Kapton substrates for 10 min. The samples obtained after electrospinning are dried at 60 °C for 30 min in a ventilated oven.

Fabrication of the ZnO nanofiber based UV sensor

The ZnO precursor is prepared by using a reported method.[24] With a vertical electrospinning setup, electrospinning is conducted at 25 kV and the distance between the needle and the collector is 20 cm. The as-electrospun nanowires are calcined at 450 °C in air for 3 h. The heating rate is 2 °C min^{-1}. The two ends of the as-prepared ZnO nanowires are connected with carbon electrodes without any package to make the UV sensor.

Acknowledgements

We gratefully acknowledge the financial support from NSFC (no. 51322203), Fok Ying Tung education foundation (no. 131044), PCSIRT (no. IRT1251), the "thousands talents" program for pioneer researcher and his innovation team, China, the Fundamental Research Funds for the Central Universities (no. lzujbky-2013-k04, lzujbky-2013-34, lzujbky-2013-230).

Notes and references

1 Z. L. Wang, *ACS Nano*, 2013, **7**, 9533.
2 Z. H. Lin, G. Cheng, L. Lin, S. Lee and Z. L. Wang, *Angew. Chem., Int. Ed.*, 2013, **52**, 12545.
3 W. Q. Yang, J. Chen, G. Zhu, J. Yang, P. Bai, Y. J. Su, Q. S. Jing, X. Cao and Z. L. Wang, *ACS Nano*, 2013, **7**, 11317.
4 Y. J. Su, Y. Yang, H. L. Zhang, Y. N. Xie, Z. M. Wu, Y. D. Jiang, N. Fukata, Y. Bando and Z. L. Wang, *Nanotechnology*, 2013, **24**, 295401.
5 F. R. Fan, Z. Q. Tian and Z. L. Wang, *Nano Energy*, 2012, **1**, 328.
6 F. R. Fan, L. Lin, G. Zhu, W. Z. Wu, R. Zhang and Z. L. Wang, *Nano Lett.*, 2012, **12**, 3109.
7 X. S. Zhang, M. D. Han, R. X. Wang, F. Y. Zhu, Z. H. Li, W. Wang and H. X. Zhang, *Nano Lett.*, 2013, **13**, 1168.
8 M. D. Han, X. S. Zhang, B. Meng, W. Liu, W. Tang, X. M. Sun, W. Wang and H. X. Zhang, *ACS Nano*, 2013, **7**, 8554.
9 S. H. Wang, L. Lin and Z. L. Wang, *Nano Lett.*, 2012, **12**, 6339.
10 G. Zhu, C. F. Pan, W. X. Guo, C. Y. Chen, Y. S. Zhou, R. M. Yu and Z. L. Wang, *Nano Lett.*, 2012, **12**, 4960.
11 L. Lin, S. H. Wang, Y. N. Xie, Q. S. Jing, S. M. Niu, Y. F. Hu and Z. L. Wang, *Nano Lett.*, 2013, **13**, 2916.
12 Z. H. Lin, G. Zhu, Y. S. Zhou, Y. Yang, P. Bai, J. Chen and Z. L. Wang, *Angew. Chem., Int. Ed.*, 2013, **52**, 5065.
13 L. Lin, Y. N. Xie, S. H. Wang, W. Z. Wu, S. M. Niu, X. N. Wen and Z. L. Wang, *ACS Nano*, 2013, **7**, 8266.
14 Y. Yang, G. Zhu, H. L. Zhang, J. Chen, X. D. Zhong, Z. H. Lin, Y. J. Su, P. Bai, X. N. Wen and Z. L. Wang, *ACS Nano*, 2013, **7**, 9461.
15 J. Chen, G. Zhu, W. Q. Yang, Q. S. Jing, P. Bai, Y. Yang, T. C. Hou and Z. L. Wang, *Adv. Mater.*, 2013, **25**, 6094.
16 Y. Yang, H. L. Zhang, Z. H. Lin, Y. S. Zhou, Q. S. Jing, Y. J. Su, J. Yang, J. Chen, C. G. Hu and Z. L. Wang, *ACS Nano*, 2013, **7**, 9213.
17 R. Lucas, T. McMichael, W. Smith and B. Armstrong, *Solar Ultraviolet Radiation: Global burden of disease from solar ultraviolet radiation*, Report no. 13, World Health Organization, Geneva, 2006.
18 P. Bai, G. Zhu, Z. H. Lin, Q. S. Jing, J. Chen, G. Zhang, J. Ma and Z. L. Wang, *ACS Nano*, 2013, **7**, 3713.
19 G. Zhu, Z. H. Lin, Q. S. Jing, P. Bai, C. F. Pan, Y. Yang, Y. S. Zhou and Z. L. Wang, *Nano Lett.*, 2013, **13**, 847.
20 D. Li and Y. N. Xia, *Adv. Mater.*, 2004, **16**, 1151.
21 R. S. Yang, Y. Qin, C. Li, L. M. Dai and Z. L. Wang, *Appl. Phys. Lett.*, 2009, **94**, 022905.
22 World Health Organization, *Global Solar UV Index: A Practical Guide*, WHO, Geneva, Switzerland, 2002.
23 G. G. Li, Z. Y. Hou, C. Peng, W. X. Wang, Z. Y. Cheng, C. X. Li, H. Z. Lian and J. Lin, *Adv. Funct. Mater.*, 2010, **20**, 3446.
24 Z. T. Zhu, L. F. Zhang, J. Y. Howe, Y. L. Liao, J. T. Speidel, S. Smith and H. Fong, *Chem. Commun.*, 2009, 2568.